J Mol Model (2009) 15:1237–1244
DOI 10.1007/s00894-009-0487-0

ORIGINAL PAPER

Computational modeling of the adsorption and $^{\bullet}$OH initiated photochemical and photocatalytic primary oxidation of nitrobenzene

Hilal S. Wahab · Andreas D. Koutselos

Received: 16 December 2008 / Accepted: 8 February 2009 / Published online: 17 March 2009

Abstract The adsorption and primary oxidation step for the photodegradation of nitrobenzene (NB) have been studied computationally using MSINDO SCF MO method. The method performs efficiently for extended surface models such as $Ti_{36}O_{90}H_{36}$. Molecular dynamics simulations have revealed that NB is linked to TiO_2 surface at the titanium ion *via* the oxygen atoms of NO_2 group. In addition, the computed vibrational density of states for the adsorbed NB molecule is in reasonably good agreement with the available experimental data and theoretical results. In order to identify the primary photochemical and photocatalytic $^{\bullet}$OH initiated photooxidation intermediates, we have employed two different theoretical approaches, frontier orbital theory and Wheland localization theory. It has been found that the *meta*- hydroxynitrocyclohexadienyl radical is energetically more favored than *para*- and *ortho*-hydroxynitrocyclohexadienyl radicals for the photochemical photolysis, whereas in the case of photocatalysis, the $^{\bullet}$OH radical attack is unselective and all three possible isomers have comparable stabilities.

Keywords Adsorption · Model calculations · Nitrobenzene · Photooxidation · Semiempirical method · Titanium oxide

H. S. Wahab (✉) · A. D. Koutselos
Laboratory of Physical Chemistry, Chemistry Department,
National and Kapodistrian University of Athens,
Zografou 15771 Athens, Greece
e-mail: hswahab@yahoo.com

Present address:
H. S. Wahab
University of Technology, School of Applied Sciences,
P.O. Box 35319, Baghdad, Iraq

Introduction

Aromatic nitro compounds are commonly used in industrial processes for manufacturing of pesticides, dyes, explosives, herbicides and drugs. As a result, they appear as contaminants in water sources, such as surface water and industrial wastewaters [1]. Nitrobenzene (NB) has been selected as a model pollutant, in the present work, because the listing of NB as a priority pollutant necessitates the study of its degradation processes. Nitrobenzene is a very toxic substance, which is readily absorbed on contact with the skin, affecting the central nervous system and causing headache, vomiting, and coma [2]. Substantial literature investigations on the treatment of NB by homogeneous and heterogeneous advanced oxidation processes have been published [3–5]. Nevertheless, although adsorption has a major role to play in the photocatalytic degradation on TiO_2, limited literature is available on the adsorption of NB. Bhatkhande et al. [2] have reported that the adsorption is affected by several factors that include the pH and composition of the aqueous systems. Palmisano et al. [3], in their partial oxidation of aromatic compounds in heterogeneous photocatalysis study, have reported ~8% adsorption for NB in the dark. Bhatkhande et al. [1] studied the photodegradation of NB using artificial UV light. The authors indicated that the degradation rate of NB is higher than that of phenol, because NB is a more strongly adsorbing species than phenol.

Although most of the studies have focused on the role of the adsorption in the photodegradation of NB, the adsorption geometries of NB onto TiO_2 surface have not yet been reported. Here, such structures will be determined by a computational method that simulates the adsorption of NB onto TiO_2 (100) surface.

Since $^{\bullet}$OH radical is a strong electrophile, the mechanistic studies have probed that hydroxycyclohexadienyl

radicals are produced as intermediates in the first oxidation steps of organic molecules [5, 6]. In addition, an on-going debate refers to whether the initial oxidation of the organic pollutant occurs on the surface of the catalyst or in the bulk of the solution [7]. Turchi and Ollis [8] have reported that the $^{\bullet}$OH radical can diffuse several hundreds of angstroms away from the surface into the bulk leading to a photochemical homogeneous phase process. On the other hand, ESR studies have shown that the $^{\bullet}$OH radical might migrate only a few atomic distances from the surface, and the $^{\bullet}$OH radical photooxidation is a surface (heterogeneous) process [9]. Accordingly, in the present work we also analyze computationally the primary steps of the oxidation of NB by $^{\bullet}$OH radical, in the homogeneous gas phase (photochemical) and on the anatase TiO_2 surface (photocatalytic).

Computational approach

The quantum chemical calculations of the heterogeneous oxidation of NB require an extended cluster for the modeling of the anatase TiO_2 (100) surface such as $Ti_{36}O_{90}H_{36}$. For this purpose, we employ the semiempirical MSINDO method that permits accurate and efficient MO calculations for many-atom configurations. The method has been extensively documented for the first-, second- and third-row main group elements and first-row transition metal elements [10–12]. The second row elements are described by a (2s, 2p) basis set and the transition metal atoms are described by pseudo minimal Slater basis set (3d, 4s, 4p). The basis functions acquire different Slater exponents in the calculations of intra- and inter-atomic integrals, as in the case of Pople 6-31G basis set. The elements of the inner shells are taken into account by Zerner pseudo potentials [13]. In addition, the new parameterization of MSINDO for first-row transition elements from Sc to Zn [12] offers a highly improved accuracy for structure and energy of transition metal compounds. Besides, MSINDO is a reliable method for studies of surface properties and further, reproduces adsorption energy values comparable to high level density functional theory calculations (14). Accordingly, the combination of reliable accuracy for structure and energy and the speed of computation for large systems make the semiempirical MSINDO a useful tool for the present study.

The dynamic studies of the cluster-substrate (TiO_2-$C_6H_5NO_2$) models are performed through isokinetic molecular dynamics (MD) simulations for 2000, 4000 and 6000 femtoseconds at 300 K, using the Nose-Hoover Chain thermostat. In the starting structure, the time step used for the simulation was one femtosecond, in order to figure out the minimum steps and shortest run time required for the adsorption process. The molecular orbital (MO) calculations have been performed at the self-consistent field (SCF) level with energy convergence accuracy better that 10^{-9} Hartree. First, the geometries of the isolated systems, substrates and clusters, as well as the cluster-substrate complex were optimized. Then the adsorption energies (E_{ads}) were calculated through [14] the following expression:

$$E_{ads} = E^{cluster-substrate} - \left(E^{substrate} + E^{cluster}\right), \quad (1)$$

where $E^{cluster\text{-}substrate}$, $E^{substrate}$ and $E^{cluster}$ are the corresponding energies for the optimized structures of the cluster-substrate system, the substrate and the cluster, respectively. The emergence of a stable system therefore would require negative E_{ads} value. All the computed energies are net values, which are already corrected toward zero point energies.

The vibrational frequencies and heats of formation are computed using the parameter NVIB=4 FULL, within MSINDO framework [15], whereas, HOMO-LUMO and their coefficients are calculated through the MOVEC keyword.

We have employed the saturated $Ti_{36}O_{90}H_{36}$ cluster model for modeling of anatase TiO_2 (100) surface, which has been used as an adsorption surface. In order to circumvent the spin localization phenomenon due to the coordinative unsaturated sites, we followed similar water saturation strategy reported in a previous study [16]. Moreover, this relatively small cluster is utilized in order to avoid excessive computer time in the subsequent adsorption calculations.

Results and discussion

Adsorption modes

The anatase TiO_2 (100) surface, which is employed here, consists of fivefold coordinated titanium Ti_{5C} atoms, Lewis acid sites, and two and three fold coordinated oxygen O_{2C} and O_{3C} atoms, Lewis base sites. Whereas, the (100) × (010)

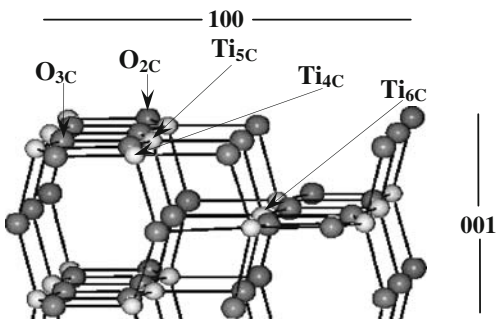

Fig. 1 The features of anatase TiO_2 (100) surface. Light spheres represent titanium atoms and the dark spheres represent oxygen atoms

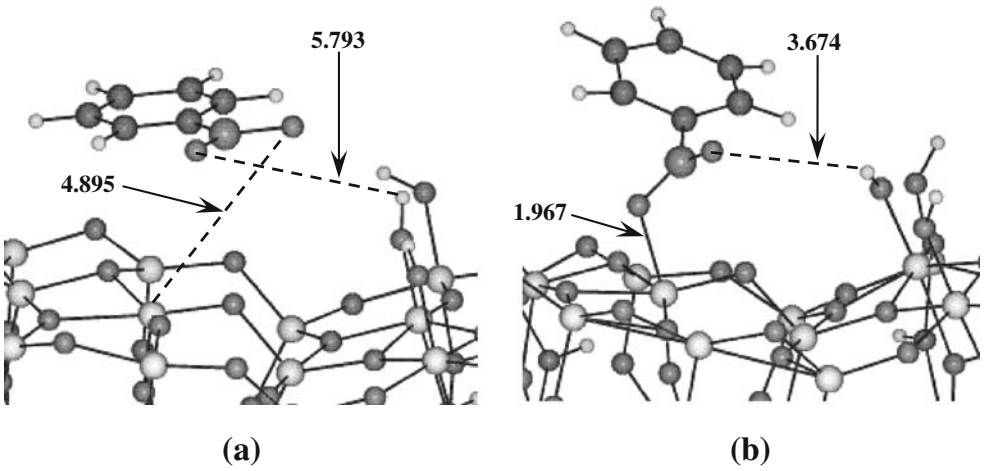

Fig. 2 MD simulation for parallel adsorption geometry; (**a**) initial structure; (**b**) minimum energy structure. Dashed lines represent distances. Ti (large light), H (small light), O (small dark), C (medium dark), N (large dark)

edge contains a fourfold coordinated titanium atom Ti_{4C}, (Fig. 1), which also acts as a Lewis acid site.

There are different ways to align the NB ring on top of the TiO_2 surface. However, we focused in this study on the parallel and perpendicular conformations, which are the most common arrangements.

The MD simulation for the parallel adsorption geometry of NB onto the anatase TiO_2 (100) surface is depicted in Fig. 2. It is explicitly shown, on the one hand, that the substrate (NB) is approaching the surface with one of the oxygen atoms of NO_2 group linking to the lattice fivefold coordinated titanium ion, preserving the parallel conformation. On the other hand, the second oxygen atom of NO_2 group has been involved in a hydrogen bonding with the surface hydroxyl group. The interesting observation in the optimization of NB molecule during adsorption simulation is the rotation of NO_2 group prior to adsorption. The phenomenon of NO_2 internal rotation has also been observed by Shlyapochnikov et al. [17], in their *ab initio* calculations for the vibrational frequencies of the C-NO_2 moiety. The same trend was observed with the perpendicular adsorption model, which is illustrated in Fig. 3. However, the plane of the aromatic ring, which preserved the vertical configuration relative to the surface upon optimization, linked to the surface lattice fivefold coordinated titanium ions *via* both oxygen atoms of NO_2 group. The NO_2 group has also rotated prior to adsorption.

The above findings, which envisage the experimental adsorption of the substrate in the dark, indicate that the main interaction between NB molecule and the surface of TiO_2 takes place through the oxygen atoms of NO_2 group rather than *via* a π-interaction with the aromatic ring. Attachment to TiO_2 (100) surface through oxygen has also been observed in a previous study for *p*-chlorophenol [18]. In addition, the adsorption of NB onto TiO_2 has been inferred by Bhatkhande et al. [2] through the large decrease in concentration of NB observed at the beginning of photocatalytic experiments.

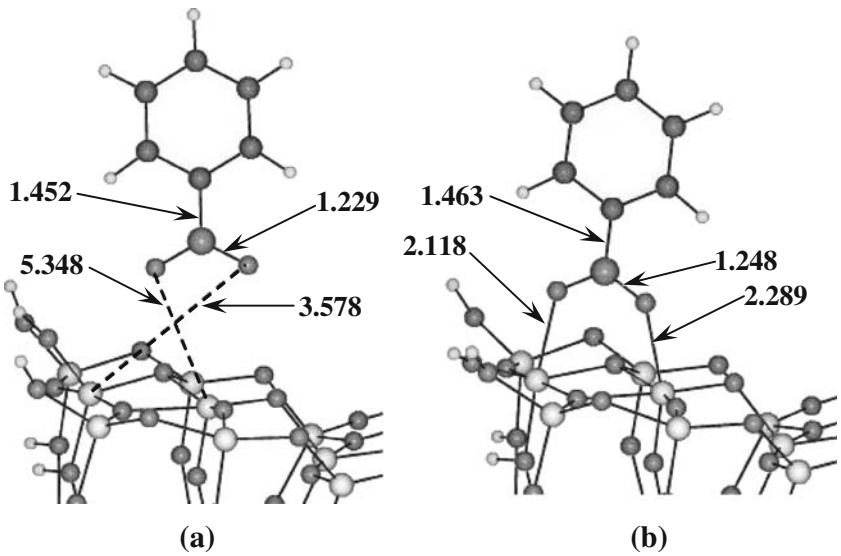

Fig. 3 MD simulation for perpendicular adsorption geometry; (**a**) initial structure; (**b**) minimum energy structure. Dashed lines represent distances. Ti (large light), H (small light), O (small dark), C (medium dark), N (large dark)

Table 1 Computed energies of the parallel and perpendicular adsorption systems

Energies	Nitrobenzene	Ti36O90H36	Parallel adsorption	Perpendicular adsorption
E(total), a.u.	−79.4961	−1579.1271	−1658.7027	−1658.7074
Zero point energy, a.u.	0.1095	0.9187	1.0212	1.0210
E(total), corrected, a.u.	−79.3866	−1578.2084	−1657.6815	−1657.6864
Binding energy, a.u.	−2.4522	−34.2838	−36.8156	−36.8202

Table 1 reveals the details of computed energies for the parallel and perpendicular adsorption systems. The lower binding energy (higher negative in magnitude) of the perpendicular adsorption conformation may highlight the possibility of its higher stability. Furthermore, as can be seen from the data in Table 2, the Löwdin net charges of the oxygen atoms of NO_2 group and surface titanium ions for the optimized perpendicular adsorption model are lower than those in the case of the optimized parallel adsorption model. This reveals explicitly the higher possibility of charge transfer, in the perpendicular geometry, for the non-bonding electron pair of the oxygen atoms into the empty d orbital of titanium atoms.

The computed E_{ads} values of both adsorption modes are found to be negative, Table 2, which indicate that the adsorption process is exothermic [19]. Further, from this table one concludes that: (a) the adsorption energy is influenced by the substrate geometry; (b) notwithstanding of longer Ti-O bonds in perpendicular adsorption mode, the higher number of linkages between the substrate and the surface lead to lower energies and consequently more stable geometries and (c) our adsorption study point to a preferential interaction, *i.e.*, energetically more favorable, between the oxygen atoms of NO_2 group and the surface of TiO_2 when the initial adsorption conformation is perpendicular. Therefore, further studies in this work were restricted to the perpendicular adsorption mode.

To provide convincing support for the proposed adsorption mechanism, the vibrational density of states (VDOS) for the model seen in Fig. 3 b, together with the free (non-adsorbed) NB molecule (as a reference) has been computed by means of their optimized coordinates and trajectories, using post-MD software within the MSINDO framework. The estimated VDOS for the reference NB molecule and the selected atoms in the adsorption model are presented in Fig. 4 a and b, respectively. The spectrum shown in Fig. 4 a includes several bands located at 1382.5, 1550 and 1571 cm^{-1}, which are assigned to NO_2 group in NB molecule. The band located at 1382.5 cm^{-1} can be assigned to the symmetric NO_2 stretching vibration and to the C-NO_2 stretching vibration, and the bands at 1550 and 1571 cm^{-1} are assigned to the asymmetric NO_2 stretching vibration. Similar bands located at 1348 and 1525 cm^{-1}, which were assigned to C-NO_2 stretching vibration and asymmetric NO_2 stretching vibration, respectively, were observed experimentally for radiolytic degradation of NB in aqueous solutions [20]. Moreover, from the *ab initio* MO calculations for NB molecule, using restricted Hartree-Fock (RHF) and Møller-Plesset (MP2) computational levels of theory [17], analogous bands located at 1391 and 1541.7 cm^{-1} have also been reported for the symmetric NO_2 and asymmetric NO_2 stretching vibrations, respectively.

The spectrum seen in Fig. 4 b reveals a shift in the bands at 1348, 1500, and 1535.5 cm^{-1}. Shift of the bands of higher intensity, particularly for the asymmetric NO_2 stretching vibrations, could be attributed to the weakening of the relevant bonds upon the adsorption process, in which the C-N and N-O bonds have become longer (Fig. 3 b). In conclusion, the above findings through MSINDO calculations confirm that the NB molecule is adsorbed to the surface *via* oxygen atoms of the NO_2 group, and the computed frequencies are in reasonably good agreement with the available experimental data and theoretical results.

Photochemical oxidation

We proceed with the study of the $^{\bullet}OH$ radical attack for the free NB molecule. The $^{\bullet}OH$ radical has been regarded as the major species responsible for the degradation of organic pollutants [7]. Similarly, from the determination of intermediate compounds generated during the first oxidation steps, mechanistic studies have shown that $^{\bullet}OH$ radicals are the species involved in the oxidation processes [3], which lead consequently, to the formation of hydroxycyclohexadienyl radicals [7].

There are several theoretical methods in the literature for the determination of the $^{\bullet}OH$ radical attack position on the

Table 2 Characteristics of nitrobenzene adsorption modes on anatase TiO_2 (100) surface

Initial Geometry	O-Ti bond (Å)	O charge (a.u.)	Ti charge(a.u.)	E_{ads} (a.u.)
Parallel	1.967	−0.4368	+1.4463	−0.0866
Perpendicular	2.118, 2.289	−0.4328, −0.4237	+1.4023, +1.3163	−0.0914

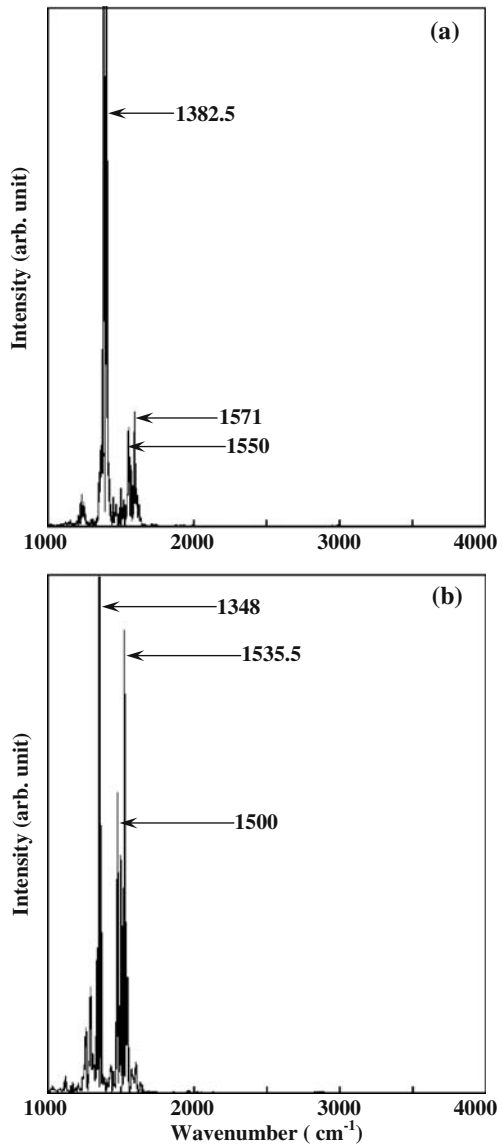

Fig. 4 The VDOS of nitrobenzene molecule adsorption on TiO_2 (100) surface; (**a**) VDOS of free nitrobenzene molecule as a reference; (**b**) VDOS of the adsorbed nitrobenzene molecule.

aromatic molecules producing hydroxycyclohexadienyl type radical [21]. Frontier orbital theory (FOT) is considered as one of these successful methods. This theory states that in electrophilic reactions, the point of •OH radical attack should be at the position of greatest electron density in the highest occupied molecular orbital (HOMO) of the molecule, whereas in the nucleophilic interaction, the attack is expected where the lowest unoccupied molecular orbital (LUMO) has the maximum electron density [22]. Another successful method is the Wheland localization approach [21, 22]. In this theory, the position of attack is assigned by the energy of the Wheland intermediates.

The HOMO and LUMO of NB molecule are pure π-molecular orbital. Its HOMO and LUMO energy levels and singly occupied molecular orbital (SOMO) of the •OH radical are schematically represented in Fig. 5. Since the •OH radical has a very low-lying SOMO, one can anticipate that in the hydroxylation of NB molecule, the interaction of the SOMO (−0.5493 a.u.) of •OH radical with the HOMO (−0.3782 a.u.) of NB molecule predominates. While, the electron transfer from •OH radical to the LUMO of NB molecule, *i.e.,* SOMO/LUMO interactions, would require higher activation energy. The values of HOMO and LUMO coefficients for the NB molecule obtained in this study are shown in Figs. 6 a and b, respectively. The HOMO coefficient values, for the photochemical degradation process, reveals the preference of the reactivity sequence as *meta-* > *ortho-* > *para-* positions with respect to the functional -NO_2 group. Hence, the electrophilic •OH radical attack follows the expected selectivity rules (*i.e.,* NO_2 is *meta*-directing group) with preference for *meta*-substitution. This computational finding is in accordance with the reported experimental observations [23] for the direct UV photodegradation of NB molecule in the presence of H_2O_2. Whereas, the LUMO coefficient values (Fig. 6 b) are greater and indicate a preference for *ortho-* and *para*-substitutions.

On the basis of the above results, one can foresee a change in substitution pattern, if the HOMO and LUMO of the aromatic molecule have different coefficient values. Eberhardt and Yoshida [22] reported that the interaction between the high-lying SOMO of nucleophilic species like O^- and N_2O^-, and the LUMO of NB molecule are predominant, whereas, the low-lying SOMO of the electrophilic •OH radical interacts with the HOMO of NB molecule. Accordingly, we expect more *ortho-, para-* and less *meta*-substitution in the case of nucleophilic primary oxidation of NB molecule in homogeneous media, while, the domination of *meta*-substitution in the case of electrophilic initial oxidation is anticipated. Also from Fig. 6 a,

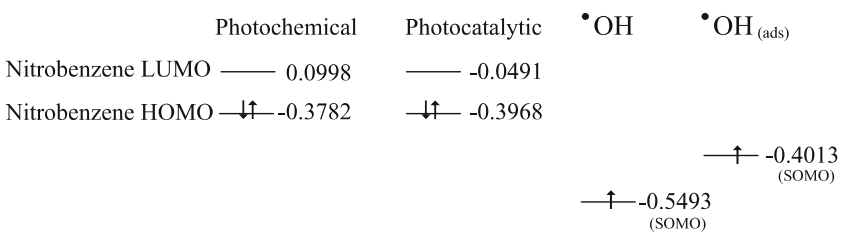

Fig. 5 HOMO - LUMO and SOMO energies in atomic units

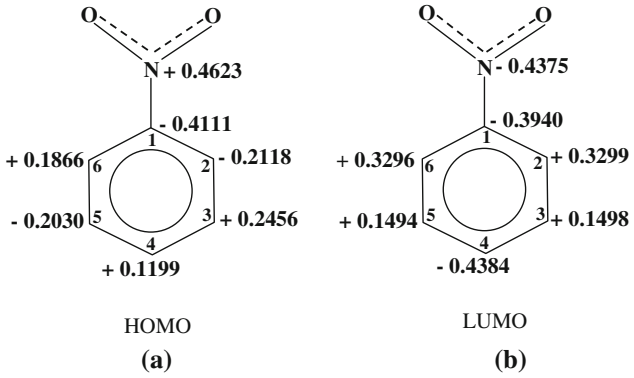

Fig. 6 HOMO and LUMO coefficients for free nitrobenzene

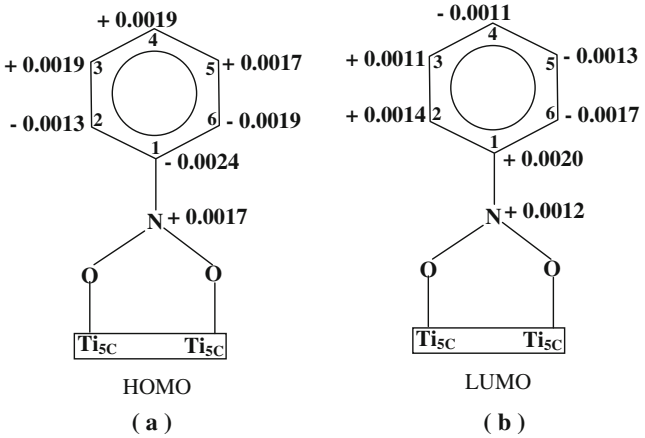

Fig. 7 HOMO and LUMO coefficients for adsorbed nitrobenzene onto TiO_2 surface

one notices the high HOMO coefficients at the nitrogen (N) and the substituted carbon (C1) atoms. This would lead one to expect attack of $^{\bullet}$OH radical in either the N or the C1 atom, however certain factors indicate for the contrary. At the substituted carbon atom, there is a steric hindrance, which may cause an increase in the activation energy of the interaction. On the other hand, pulse radiolysis studies on aqueous NB solution have shown attack at the ring: This behavior could be ascribed to the solvation shell surrounding the nitro group in aqueous solution [22]. With the aromatic skeleton remaining unchanged during the calculations for the hydroxynitrocyclohexadienyl radicals, we have obtained energies, and thus the relative stability of the species, as well as heats of formation, as presented in Table 3. In line with the Wheland approach and from the data shown in Table 3, it could be concluded that the stability of the Wheland intermediates follows the sequence of *meta*- > *ortho*- > *para*-hydroxynitrocyclohexadienyl radical, despite the energy differences being small. The preference of *ortho*-isomer over *para*-isomer is attributed to the intramolecular hydrogen bonding effect between nitro group (O atom) and the hydroxyl group (H atom). This phenomenon, *ortho*-effect, is in congruence to other studies [6, 23]. Thus, both FOT and Wheland approach resulted in similar prediction for the reactivity sequence, with the *meta*-position attack predominating. The stability of *meta* - hydroxylated radical over *ortho* and *para* radicals, in the presence of electron withdrawing group, i.e., NO_2, is mainly ascribed to the resonance structures [24, 25].

Finally, we observe from Table 3 that the SOMO energy of the *meta*-adduct lies below those of the *ortho*- and *para*-adducts, confirming the relative stability of the *meta*-isomer.

Photocatalytic oxidation

After ensuring the description of the initial oxidation of free NB molecule by the $^{\bullet}$OH radical through the present method, we proceed to analyze the photocatalytic degradation of adsorbed NB molecule. As in the previous case, the SOMO (−0.4013 a.u.) of the adsorbed $^{\bullet}$OH radical lies close to the HOMO (−0.3968 a.u.) of the adsorbed NB molecule, Fig. 5, revealing the possibility of heterogeneous photolysis on the TiO_2 surface.

The computed HOMO and LUMO coefficients for the adsorbed NB molecule (Fig. 3 b) on the photocatalyst surface are illustrated in Fig. 7a and b, respectively. The average HOMO and LUMO coefficients values at the ring positions, for the *ortho*- (C2 and C6), *meta*- (C3 and C5) and *para*- (C4) positions with respect to the functional

Table 3 MSINDO calculations on hydroxynitrocyclohexadienyl radicals[a]

	1,2	1,3	1,4
E (total), a.u.	−95.891	−95.894	−95.891
ΔE, kJ mol^{-1}	7.875	0.000	7.875
ΔH_f, kJ mol^{-1}	−12.508	−12.958	−11.826
E (SOMO), a.u.	−0.3401	−0.3411	−0.3395

[a] The numbers in the column headings indicate the position of the NO_2 and OH group, respectively.

Table 4 MSINDO calculations on the adsorbed hydroxynitrocyclohexadienyl radicals[a]

	1,2	1,3	1,4
E (total), a.u.	−1675.191	−1675.189	−1675.192
ΔE, a.u.	2.625	7.875	0.000
ΔH_f, kJ mol^{-1}	−9927.9	−9926.5	−9927.7
E (SOMO), a.u.	−0.3950	−0.3856	−0.3921

[a] The numbers in the column headings indicate the position of the NO_2 and OH group, respectively.

$-NO_2$ group, are all small and comparable in comparison to the foregoing photochemical oxidation process. Furthermore, the computation of the total energies and heats of formation, for the adsorbed hydroxynitrocyclohexadienyl radical intermediates, has also exhibited (Table 4) comparable values. Again, both FOT and Wheland approach resulted in similar prediction for the reactivity of the aromatic ring positions.

Based on the above results, it can be inferred that the differences in the isomer distribution pattern, *i.e.,* the reactivity of *para*-, *meta*- and *ortho*-positions, for the photocatalytic oxidation of NB molecule in comparison to that for the photochemical oxidation are ascribed to the adsorption process. Accordingly, the interaction between the slightly positively charged TiO_2 surface and the non-bonding electron pair of the NO_2 oxygen atoms results in a variation of the charge distribution over the benzene ring and consequently, modifications in the reactivity of $^{\bullet}OH$ radical attacking positions are possible.

The occurrence of all the three monohydroxylated isomers, as photocatalytic initial oxidation products, in comparable values is in good agreement with the experimental outcomes [2, 3]. Furthermore, this computational finding indicates that the electrophilic and nucleophilic attacks on the adsorbed NB molecule are unselective.

Based on these results and from the mechanistic point of view, the computational characterization of the photooxidation intermediate products is a useful source of information to elucidate the controversial organic pollutants photooxidative degradation pathways.

Conclusions

The adsorption of nitrobenzene onto TiO_2 surface has been found to be favored energetically through molecular calculations using the MSINDO computational method. The optimization of parallel and perpendicular conformations of NB molecule relative to the surface has resulted in a linkage of the molecule to the surface titanium ion *via* oxygen atoms of NO_2 group with different stabilities.

In the case of photochemical oxidation, the $^{\bullet}OH$ radical attack follows the expected selectivity rules, in which the *meta*-isomer is energetically more favorable than *para*- and *ortho*-isomers. While in the case of photocatalytic oxidation, the attack is unselective and all three isomers have comparable stabilities.

Acknowledgments One of the authors (H. S. Wahab) warmly thanks the Greek Ministry of Education and Religious Affairs for the award of a research fellowship and the International Institute of Education/SRF for supporting a postdoctoral stay. The work was partially supported by the Research Account of the University of Athens, under the grant KA: 70/4/6482.

References

1. Bhatkhande DS, Kamble SP, Sawant SB, Pangarkar VG (2004) Photocatalytic and photochemical degradation of nitrobenzene using artificial ultraviolet light. Chem Eng J 102:283–290
2. Bhatkhande DS, Pangarkar VG, Beenackers AACM (2003) Photocatalytic degradation of nitrobenzene using titanium dioxide and concentrated solar radiation: chemical effects and scaleup. Water Res 37:1223–1230
3. Palmisano G, Addamo M, Augugliaro V, Caronna T, Di Paola A, Lopez EG, Loddo V, Marci G, Palmesano L, Schiavello M (2007) Selectivity of hydroxyl radical in the partial oxidation of aromatic compounds in heterogeneous photocatalysis. Catal Today 122:118–127
4. Priya MH, Madras GJ (2006) Photocatalytic degradation of nitrobenzenes with combustion synthesized nano-TiO_2. Photochem Photobiol A: Chem 178:1–7
5. Li QR, Gu CZ, Di Y, Yin H, Zhang JY (2006) Photodegradation of nitrobenzene using 172 nm excimer UV lamp. J Hazard Mater B 133:68–74
6. Albarran G, Schuler RH (2005) Concerted effects of substituents in the reaction of $^{\bullet}OH$ radicals with aromatics: The cresols. J Phys Chem A 109:9363–9370
7. Canle ML, Santaballa JA, Vulliet EJ (2005) On the mechanism of TiO_2-photocatalyzed degradation of aniline derivatives. Photochem Photobiol A: Chem 175:192–200
8. Turchi CS, Ollis DF (1990) Photocatalytic degradation of organic water contaminants: Mechanisms involving hydroxyl radical attack. J Catal 122:178–192
9. Helz GR, Zepp RG, Crosby DG (1994) Aquatic and surface photochemistry. Lewis, Boca Raton
10. Ahlswede B, Jug K (1999) Consistent modifications of SINDO1: I. Approximations and parameters. J Comput Chem 20:563–571
11. Ahlswede B, Jug K (1999) Consistent modifications of SINDO1: II. Applications to first- and second-row elements. J Comput Chem 20:572–578
12. Bredow T, Geudtner G, Jug K (2001) MSINDO parameterization for third-row transition metals. J Comput Chem 22:861–887
13. Zerner MC (1972) Removal of core orbitals in 'valence orbital only' calculations. Mol Phys 23:963–978
14. Homann T, Bredow T, Jug K (2004) Adsorption of small molecules on the anatase (1 0 0) surface. Surf Sci 555:135–144
15. Wahab HS, Bredow T, Aliwi SM (2008) Computational investigation of the adsorption and photocleavage of chlorobenzene on anatase TiO_2 surfaces. Chem Phys 353:93–103
16. Wahab HS, Bredow T, Aliwi SM (2008) MSINDO quantum chemical modeling study of water molecule adsorption at nano-sized anatase TiO_2 surfaces. Chem Phys 354:50–57
17. Shlyapochnikov VA, Khaikin LS, Grikina OE, Bock CW, Vilkov LV (1994) The structure of nitrobenzene and the interpretation of the vibrational frequencies of the C–NO_2 moiety on the basis of ab initio calculations. J Mol Struct 326:1–16
18. Wahab HS, Bredow T, Aliwi SM (2008) Computational modeling of the adsorption and photodegradation of 4-chlorophenol on anatase TiO_2 particles. THEOCHEM 863:84–90
19. Serpone N, Pelizzetti E (1989) Photocatalysis, fundamentals and applications. Wiley, New York
20. Zhang SJ, Jiang H, Li MJ, Yu HQ, Yin H, Li QR (2007) Kinetics and mechanisms of radiolytic degradation of nitrobenzene in aqueous solutions. Environ Sci Technol 41:1977–1982
21. San N, Hatipoglu A, Koçtürk G, Çinar Z (2002) Photocatalytic degradation of 4-nitrophenol in aqueous TiO_2 suspensions: Theoretical prediction of the intermediates. J Photochem Photobiol A: Chem 146:189–197

22. Eberhardt MK, Yoshida M (1973) Radiation-induced homolytic aromatic substitution. I. Hydroxylation of nitrobenzene, chlorobenzene, and toluene. J Phys Chem 77:589–597
23. Chen PC, Chieh YC, Tzeng SC (2003) Density functional calculations of the heats of formation for various aromatic nitro compounds. THEOCHEM 634:215–224
24. Rodriguez M, Kirchner A, Contreras S, Chamarro E, Esplugas S (2000) Influence of H_2O_2 and Fe(III) in the photodegradation of nitrobenzene. J Photochem Photobiol A: Chem 133: 123–127
25. March J (1992) Advanced organic chemistry-reactions, mechanisms and structure, 4th edn. Wiley, New York